

Fabrication, Characterization and NH₃ Sensing Properties of Zinc Supported TiO₂ Doped Polypyrrole Nanocomposite Thin Films

ANAND PATIL^{1,*} and NIRDOSH PATIL²

¹Department of Chemistry, PDA College of Engineering, Kalaburagi-585102, India

²Department of Chemistry, Sharnbasva University, Vidya nagar, Kalaburagi-585103, India

*Corresponding author: E-mail: patil5chemist@gmail.com

Received: 10 August 2022;

Accepted: 11 October 2022;

Published online: 25 November 2022;

AJC-21054

A series of conductive and porous Zn/TiO₂ doped polypyrrole (PPy) nanocomposites thin films were prepared by adding Zn/TiO₂ (5, 10, 15, 20 and 25 wt.%) in an aqueous solution of polypyrrole using a chemical oxidative polymerization process at room temperature. The prepared Zn/TiO₂-PPy films were characterized by electrical resistivity by two probe techniques, Fourier transform infrared (FTIR) spectroscopy, X-ray diffraction (XRD) and scanning electron microscopy (SEM). The surface morphology of Zn/TiO₂-PPy films has found significant influence on the gas sensing properties. Results from FTIR and XRD verified the structural formation of Zn/TiO₂-PPy films from the pyrrole monomer. When the amount of Zn/TiO₂ increased, the optical absorption in visible (500-700 nm) and UV (200-400 nm) regions decreases, according to an analysis of the optical characteristics of all tested films. The NH₃ gas was used to examine the prepared nanocomposites thin films' sensing properties.

Keywords: Ammonia, Titanium dioxide, Polypyrrole, Porous films.

INTRODUCTION

In a wide range of applications, including environmental energy and digital programmes, semiconductors have been extensively studied [1]. Consequently, there has been a lot of interest in the development of these materials to improve their physical characteristics. Since, it has so many applications and is so reasonably priced, titanium oxide (TiO₂) has become one of the most research in the semiconductors field [2]. Additionally, TiO₂ has been utilized as an useful and photoanode of sensitized solar cells among the numerous semi-conductor materials used [3,4] and due to its desirable characteristics, which include low cost, low toxicity, a high degree of oxidative strength and little biological or chemical activity [5]. Due to the high band gap of TiO₂, there are several challenges when using it for photovoltaic activities, such as a damaging UV source. As a result, the use of titanium oxide in visible sunlight is strictly regulated. To form a very rapid electron-hole pair, for instance, pure TiO₂ without any impurities needs a lot of light energy, which reduces the photocatalytic activity under visible light with low energy [6]. When impurities and dopants are present,

TiO₂'s characteristics might change. Doping TiO₂ with Sn and Zr can improve its electrical and optical properties [7,8].

The photocatalytic activity of TiO₂ can be increased by doping it with metals, which can lead to fascinating phase transitions, such as the change from anatase to rutile [9,10]. It is challenging to find alternative metals that can improve the features of TiO₂, such as its structural and dielectric capabilities and to promote its phase change. To enhance the photovoltage characteristics of TiO₂, Zn has caught the attention of several research groups [11,12]. The prospective applications of this material were compromised by the complicated procedures these investigations used to prepare the substance chemically. TiO₂ nanoparticles doped with traces of zinc have a range of important optical uses for research and business in addition to its activity as a powerful antibacterial substance, thus it is imperative to find a way for their rapid, environmentally friendly and more effective manufacture [13]. Zinc doped TiO₂ has unique chemical and physical features because it creates an n-type dopant that assists in electron transport. Additionally, the doping approach helps control the material's light band gap. TiO₂ was commonly employed in photocatalysis to accele-

rate photoconduction as compared to undoped TiO₂ [14]. In order to detect harmful gases like NH₃, this work investigates the conducting and gas sensing behaviour of Zn/TiO₂ doped polypyrrole nanocomposites.

EXPERIMENTAL

Titanium oxide and zinc chloride (both 99.99% procured from S.D. Fine Chemicals, India) were used in the preparation of metal oxide nanocomposites. Ammonium persulphate and pyrrole monomer (mPPy) (Sigma-Aldrich, USA). The synthesis was carried out utilizing a simple wet impregnation method and all the aqueous solutions were prepared with deionized water.

Sample preparation: The wet impregnation method was used to make Zn/TiO₂ [15]. A 1.0 g of TiO₂ (undoped) dissolved in 3 mL of deionized water before being added, along with 0.014 g of Zn (~ 65 g/mol) in ZnCl₂ (about 136 g/mol), before 5 wt.% of ZnCl₂ was added. A steady addition of the produced solution to the combined TiO₂ solution was made. The mixture was then dried in 120 °C after being left at room temperature for 24 h. The sample was then finely crushed into a pellet by a hydraulic die-set ket.

Synthesis of polypyrrole (PPy): Chemical oxidative polymerization was used in the synthesis of polypyrrole by mixing equimolar pyrrole (0.1 M) and HCl in aqueous medium followed by the addition of ammonium persulphate (0.2 M) dropwise at 0-5 °C in an ice bath by agitation for 12 h followed by polymerization reaction about 6 h while being constantly agitated. The PPy precipitate was collected, washed repeatedly with a solution of ethanol, deionized water and then dried in a vacuum for 24 h at 60 °C before being pulverized into a powder.

Fabrication of Zn/TiO₂ doped polypyrrole nanocomposite thin films: Polypyrrole (PPy) was dissolved in deionized water at 90 °C and then diluted to 10 wt.%. After being further crushed to a size lower than 50 nm, the Zn/TiO₂ powder was mixed with the PPy solution. The homogeneous slurry was cast on a Teflon petridish and allowed to solidify at room temperature, resulting in the formation membrane with a thickness of around 0.2 to 0.5 nm. The membrane was then stored in a dry atmosphere after being dried for 24 h at 60 °C. The wet impregnation method was used to construct different PPy-Zn/TiO₂ composite by doping different compositions of Zn/TiO₂ (5, 10, 15, 20 and 25%) into an aqueous solution of polypyrrole.

Characterization: The crystallinity of synthesized PPy-Zn/TiO₂ polymer nanocomposite films was investigated using an X-ray diffractometer (Ultima IV Japan) with CuK α radiation ($\lambda = 1.5405 \text{ \AA}$) at 40 mA and 40 kV with a scanning speed of 0.02 per second. The chemical bonding was investigated using FTIR spectroscopy and a Spectrum RXI make-model instrument from Perkin-Elmer. Using a 120 kV-operating scanning electron microscope (SEM, JSM-6360LV, Japan), the morphological characteristics of the films were investigated. A programmable Keithley source metre was used to examine the films' current-voltage (I-V) properties (Keithley 2636A)

Gas sensing measurements: Ammonia gas was used to conduct probing operations. Digital multimeters were used to measure resistance, an alumel-chrome thermocouple and digital thermometer were used to measure the temperature of the micro heater utilizing a gas sensor unit. In order to maintain a constant room temperature, a current supply of 12.5 V to the heater was given. The air resistance of the sensor was then calculated. Following the chamber's filling with a predefined amount of ammonia gas, the steady loss of sensor resistance was monitored. Once the bottle has been opened and the minimal continuous resistance value has been established, the sensor was placed outside in the open air [16].

RESULTS AND DISCUSSION

FT-IR studies: The FT-IR spectra of pure PPy and PPy-Zn/TiO₂ nanocomposites are shown in Fig. 1. The stretching vibration of C=C and C-C in the pyrrole ring is attributed to the band at 1560 cm⁻¹ and the weak band at 1470 cm⁻¹ [17,18]. The IR spectra of PPy exhibit the distinctive C-N and C-H stretching vibrations of pyrrole at wavelengths of 1202 cm⁻¹ and 1051 cm⁻¹, respectively [19]. The C-H in-plane deformation modes are related to the absorption at 1317 cm⁻¹ [20]. The band found at 920 cm⁻¹ and 677 cm⁻¹, respectively, may be brought on by polymer N-H vibration and out-of-plane ring deformation [21]. A considerable attenuation of the peak in the FT-IR spectrum of PPy-Zn/TiO₂ nanoparticle composites suggests that each nanoparticle is coated with PPy. The pyrrole ring's band at 1565 cm⁻¹ and 1475 cm⁻¹ caused by the stretching modes of C=C and C-C has vanished and a broad band has instead emerged at 1530 and 1490 cm⁻¹ in concentrations of 10% and 20% of PPy-Zn/TiO₂ nanoparticle, respectively. The metal oxide bond caused the peak to appear at higher frequen-

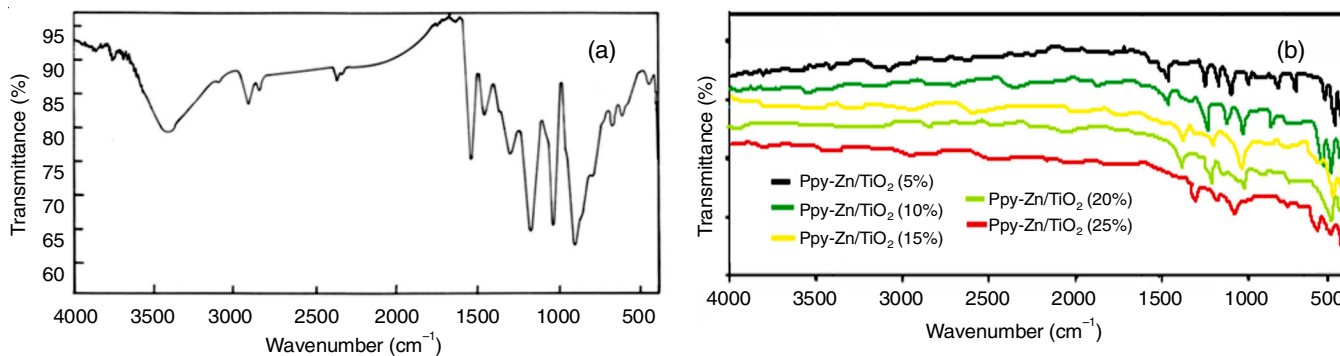


Fig. 1. IR spectra of (a) polypyrrole films and (b) PPy-Zn/TiO₂ thin films

cies between 1322 and 1290, 1210-1190 and 1060-1042 cm⁻¹, with a broad peak at 890 cm⁻¹. These notable alterations are related to a chemical reaction between PPy and Zn/TiO₂ nanoparticles, which is attributed due to the better conjugation or chain length.

XRD studies: A large peak in Fig. 2a, centred around $2\theta = 18-30^\circ$ suggests that polypyrrole is amorphous. Fig. 2b displays the XRD spectrum for pure TiO₂ and Zn doped TiO₂ (Zn/TiO₂). The typical X-ray diffraction patterns for the PPy-Zn/TiO₂ composite samples are shown in Fig. 2c. The observed diffraction peaks in the recorded XRD patterns matched the typical Zn/TiO₂ polycrystalline patterns.

Additionally, when Zn²⁺ was added to TiO₂ matrix, the diffraction peaks for Zn doped TiO₂ increase stronger, showing the generated (Zn/TiO₂) is well crystalline [22]. In comparison to TiO₂ that has not been doped with Zn, the XRD peaks for Zn doped TiO₂ exhibit a large and discernible shift towards high diffraction angles. The Zn/TiO₂ particles are highly scattered and too tiny (Fig. 2c). Additionally, the Zn/TiO₂ doped poly-

pyrrole diffraction peaks become more intense with the addition of Zn/TiO₂, indicating the well-crystalline character of the generated PPy-Zn/TiO₂ composite films. As Zn/TiO₂ is doped into polypyrrole, the XRD peaks shift significantly and visibly in favour of a high diffraction angle when compared to undoped polypyrrole. The XRD pattern also suggested that as dopant (Zn/TiO₂) percentage increases the sharpness of the peaks increases, hence composite materials change from amorphous to crystalline nature as dopant (Zn/TiO₂) concentration increases in polypyrrole matrix. This implies that the interplanar spacing decreases as dopants are added. This would increase the bond overlap by bringing the chains together and improving the interaction of the dopants. The recent study found that this may result in a rise in conduction.

Morphology studies: The SEM images for the composite films made of PPy-Zn/TiO₂ and Zn/TiO₂ are shown in Fig. 3. The SEM clearly distinguishes between the doped and undoped sample's microstructures. In general, undoped PPy has a greater granular structure than the doped one. The diameters of the

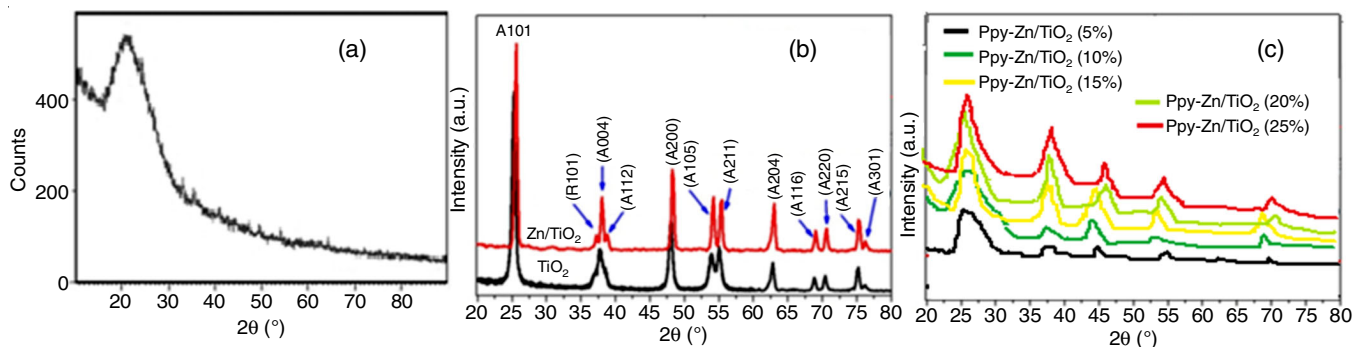


Fig. 2. XRD patterns of (a) polypyrrole, (b) undoped TiO₂ and Zn/TiO₂ and (c) PPy-Zn/TiO₂ samples

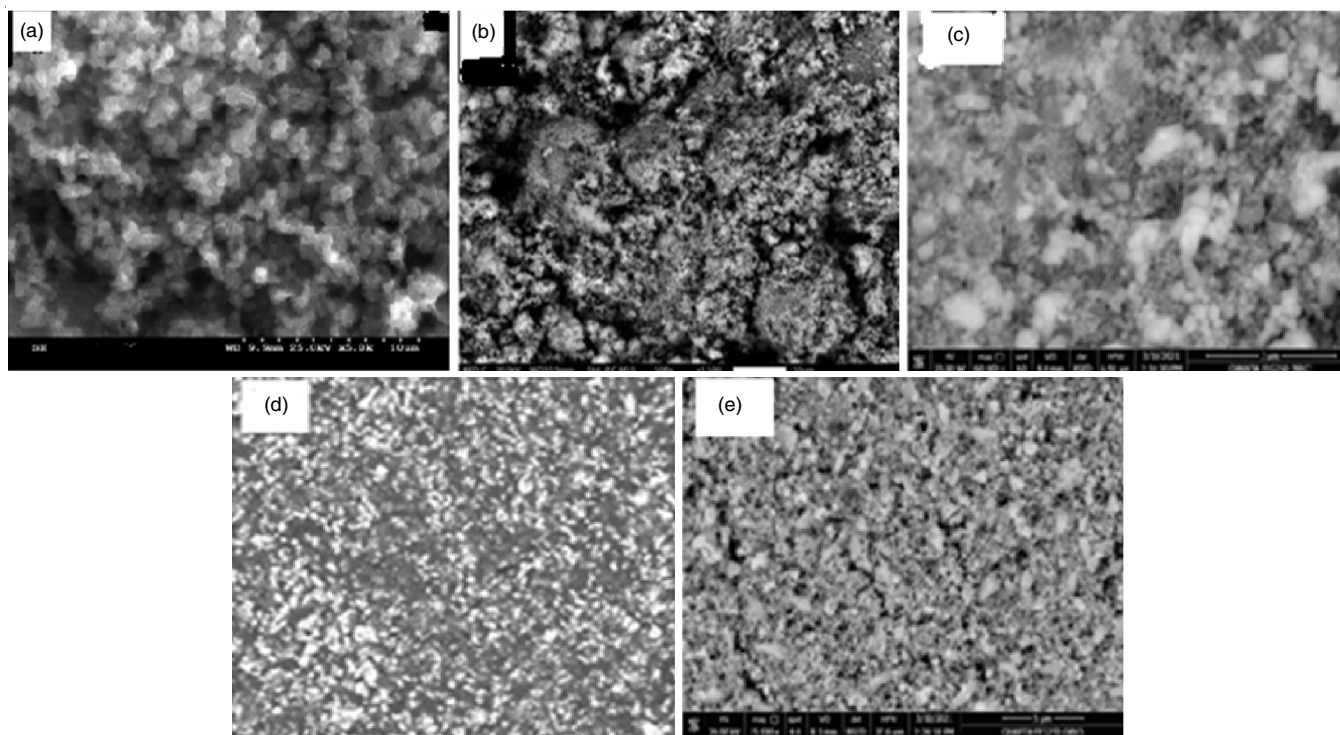


Fig. 3. SEM images of (a) PPy, (b) Zn/TiO₂, (c) PPy-Zn/TiO₂ (5%), (d) PPy-Zn/TiO₂ (10%) and (e) PPy-Zn/TiO₂ (20%)

granules were discovered to vary when dopants were utilized during the polymerization with polypyrrole. The PPy-Zn/TiO₂ films have a completely different morphology from the doped PPy. For instance, the microscopic Zn/TiO₂ particles that diffused into the layer of PPy combine to form semi-spherical structures or grains (Fig. 3). A thorough examination revealed the appearance of tiny black holes or cavities in the microstructures of PPy-Zn/TiO₂ composites, due to the emergence of comparable holes associated to the order-disorder transition in TiO₂ [23]. These morphological characteristics are thought to be beneficial for gas sensing applications.

Optical properties: The optical properties of each sample were examined in the 300-1800 nm wavelength range. The Zn/TiO₂ and PPy-Zn/TiO₂ films' optical transmission (T) spectra are shown in Fig. 4a. The reduced transmittance of the films with greater PPy-Zn/TiO₂ doping concentrations is due to an increase in photon scattering caused by the generated films' increased surface roughness [24]. Fig. 4 shows the optical absorption coefficient (α) of PPy-Zn/TiO₂ films with various Zn/TiO₂ doping contents (b). Beer-law Lambert's [25] provides an estimation of the absorption coefficient as follows:

$$\alpha = \ln\left(\frac{1}{T}\right)\left(\frac{1}{d}\right)$$

where T is the transmittance and d is the film thickness. A film without Zn/TiO₂ has a thickness of 550 nm and films doped with various amounts of Zn/TiO₂ have a thickness of 580 nm. It has been found that as the Zn/TiO₂ proportion rises, (α) increases while the wavelength (λ) drops. According to the association between incident photon energy (h) and absorption coefficient (α), the direct allowed energy band gap (E_g) of PPy-Zn/TiO₂ samples has been computed:

$$\alpha h\nu = A(h\nu - E_g)^n$$

As shown in Fig. 4c, the optical band gap (E_g) value was computed by projecting the straight line segment of the curve to the (h) axis. The results show that as Zn/TiO₂ doping levels rise, the optical band gap rises as well, which is consistent with differences in particle size. A well-known quantum confinement phenomenon known as the Burstein-Moss effect on band gap broadening causes the band gap to expand by reducing the particle size in addition to when the quantity of doping increases [126,27]. Additionally, structural disturbance in the

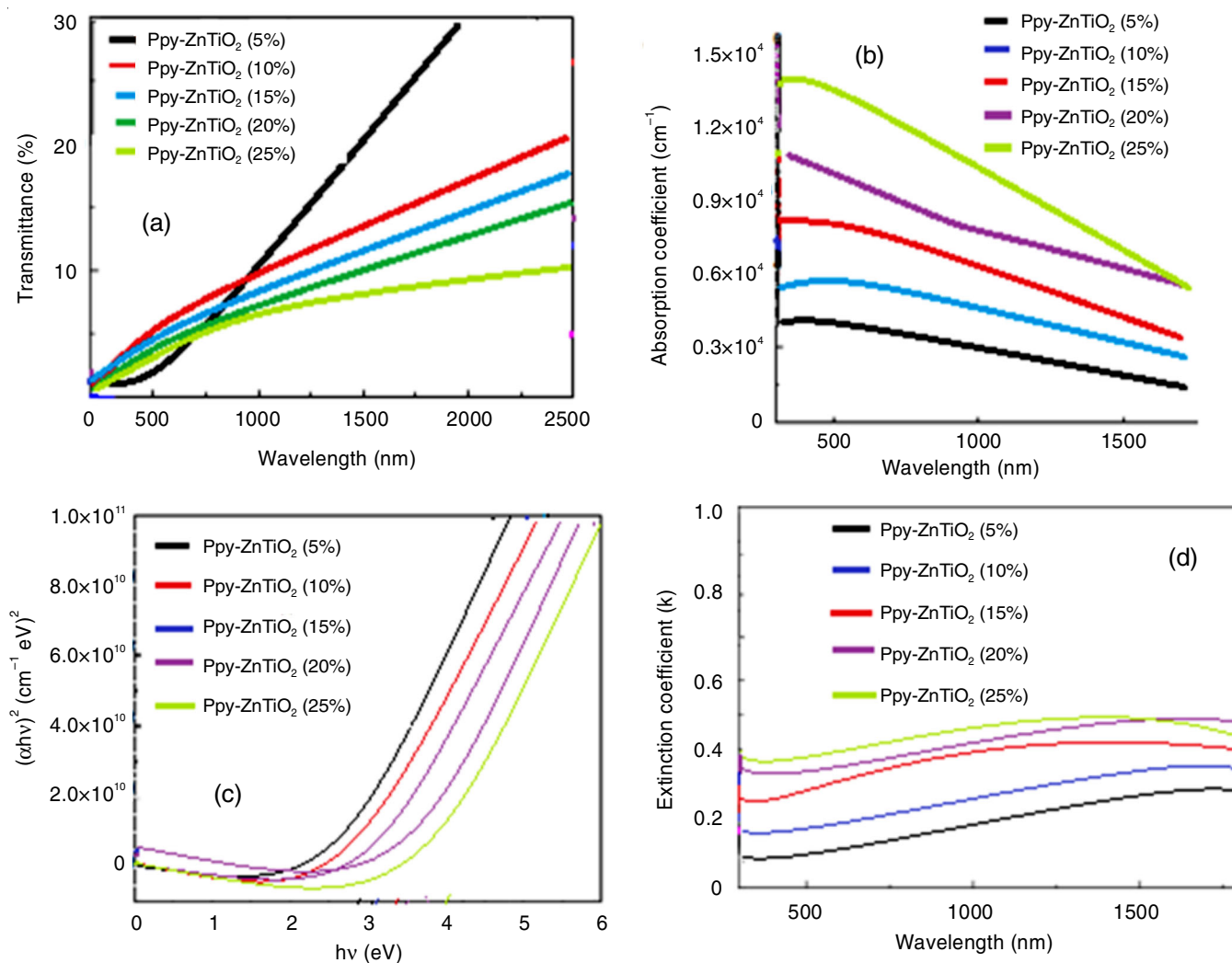


Fig. 4. (a) Relation between transmission and wavelength (nm); (b) absorption coefficient vs. wavelength (nm); (c) $(\alpha h\nu)^2$ versus $h\nu$ and (d) Extinction coefficient against wavelength

lattice may alter the distribution of mid-level energy levels between the band's gaps, changing the E_g values. The rise in E_g suggests that PPy-Zn/TiO₂ films might be applied to optoelectronic components. The extinction coefficient (k) ratio demonstrates how quickly light intensity decreases as it passes through a substance. In Fig. 4d, the connection between k and wavelength is depicted, showing that k increased as the wavelength and Zn/TiO₂ content increased.

Electrical conductivity: As shown in Table-1, the conductivity of PPy and the doped samples in pelletized powder is marginally lower than that of PPy films. As a result of the numerous kinds of structural problems that exist in PPy chains, which have a significant impact on the mobility of charge carriers and ultimately, the conductivity of the polymer. Because Zn/TiO₂ changes the conducting network of PPy chains and introduces an ordered arrangement of the macromolecular chains, it will increase conductivity when added to the backbone of PPy [28].

Sample name	Conductivity (S/cm)
PPy	2.55×10^{-3}
PPy-Zn/TiO ₂ (5%)	3.10×10^{-2}
PPy-Zn/TiO ₂ (10%)	4.27×10^{-2}
PPy-Zn/TiO ₂ (15%)	5.65×10^{-2}
PPy-Zn/TiO ₂ (20%)	6.69×10^{-2}
PPy-Zn/TiO ₂ (25%)	7.58×10^{-2}

Gas sensor: All of the Zn/TiO₂ doped polypyrrole samples were examined for ammonia gas detection. A typical graph of current *versus* time for polypyrrole generated following exposure to ammonia gas is shown in Fig. 5. All samples were tested three times to check the repeatability of the samples' absorption and desorption processes. The I vs. time curves for the second and third cycles to be somewhat different from the first cycle. This is possible because the desorption process took longer than expected to complete.

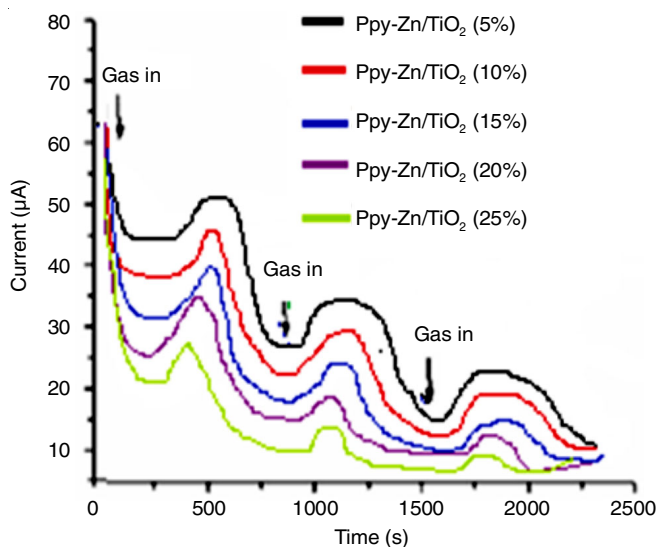


Fig. 5. Response of different PPy-Zn/TiO₂ samples towards ammonia gas

The sensitivity factor was calculated using the following equation:

$$S = \frac{R_g - R_o}{R_o}$$

where R_g and R_o are resistances with gas and without gas (in air), respectively [29,30].

Comparison studies: For both pure PPy and PPy doped with Zn/TiO₂, it was shown that different materials responded to ammonia gas in different ways. These tests revealed that a drop in current was observed when ammonia gas was exposed to Zn/TiO₂ doped PPy that had been doped with varied weight percents of Zn/TiO₂ dopants. These Zn/TiO₂ doped PPy have higher electrical conductivity than pure PPy, which shows a significant amount of charge carriers at high doping levels. Ammonia cannot create more charges because the charge density is already higher; instead, it lowers the effective charge. Therefore, under this situation, the conductivity of polypyrrole will decrease, as has actually been shown in present research. To sum up, the metal nanoparticles can improve the sensing properties of conducting polymers, mainly due to the following reasons: firstly, the introduction of metal nanoparticles changes the conductivity of polymers. Secondly, certain kinds of metal nanoparticles show a chemical affinity for specific gas substances and metal nanoparticles as chemical receptors enhance the selectivity of sensors. Last, the effective surface area of nanocomposites interacting with target gas is increased by introducing nano metals into conductive polymers. Several sensors based on the hybrid system of conducting polymers and metal oxides developed recently and their main sensing properties are summarized in Table-2. It was observed that as dopant (Zn/TiO₂) concentration increases the response of the PPy-Zn/TiO₂ composites were also increases.

Metal oxide	Conc. (ppm)	Response	Response/recovery time (s)	Ref.
SnO ₂	0.1	57	18-30	[31]
Zn ₂ SnO ₄	100	82.1	26-35	[32]
ZnO	0.5	21	256-370	[33]
Au	100	1.35	20-40	[34]
AgSnO ₂	0.02	–	–	[35]
AuTiO ₂	0.02	3.2	–	[35]
Zn/TiO ₂ (5%)	100	65	–	Present study
Zn/TiO ₂ (10%)	100	77	–	
Zn/TiO ₂ (15%)	100	79	–	
Zn/TiO ₂ (20%)	100	82	–	
Zn/TiO ₂ (25%)	100	85	–	

Conclusion

In this work, PPy-Zn/TiO₂ polymer nanocomposite thin films were prepared by chemical oxidation method. Strong peak attenuation in the FT-IR spectrum of PPy-Zn/TiO₂ nanocomposites suggests that each nanoparticle is successfully coated with polypyrrole (PPy). According to an XRD analysis, the diffraction peaks for Zn/TiO₂ doped polypyrrole grow more

strong upon insertion into the polypyrrole matrix, indicating the well-crystalline character of the obtained PPy-Zn/TiO₂ nanocomposite films. The SEM studies revealed that microscopic black holes or cavities in the microstructures of the PPy-Zn/TiO₂ composite is similar to the formation of such holes associated with the order-disorder transition in Zn/TiO₂. Increased Zn/TiO₂ doping ratios result in a rise in the optical band gap, which is correlated with changes in particle size. The conductivity measurement showed that the modification of chain's conducting network by the addition of Zn/TiO₂ to the PPy chain's backbone will boost conductivity. All of the Zn/TiO₂ doped polypyrrole samples were examined for NH₃ gas detection. It was shown that the responsiveness of PPy-Zn/TiO₂ composites increased as dopant (Zn/TiO₂) concentration increased.

ACKNOWLEDGEMENTS

The authors are thankful to Dr. Sharanabaswappa Appa, President, Sharanbasveshwar Vidya Vardhak Sangha, Kalaburagi, Dr. Anilkumar Bidve, Registrar and Dr. Laxmi Patil, Dean, Sharnbasva University, Kalaburagi, India, for their constant support and encouragement.

CONFLICT OF INTEREST

The authors declare that there is no conflict of interests regarding the publication of this article.

REFERENCES

- S.K. Tripathy and A. Pattanaik, *Opt. Mater.*, **53**, 123 (2016); <https://doi.org/10.1016/j.optmat.2016.01.012>
- A.J. Haider, R.H. AL- Anbari, G.R. Kadhim and C.T. Salame, *Energy Procedia*, **119**, 332 (2017); <https://doi.org/10.1016/j.egypro.2017.07.117>
- S. Sen, S. Mahanty, S. Roy, O. Heintz, S. Bourgeois and D. Chaumont, *Thin Solid Films*, **474**, 245 (2005); <https://doi.org/10.1016/j.tsf.2004.04.004>
- J. Deng, M. Wang, J. Fang, X. Song, Z. Yang and Z. Yuan, *J. Alloys Compd.*, **791**, 371 (2019); <https://doi.org/10.1016/j.jallcom.2019.03.306>
- R. Foulady-Dehaghi and M. Behpour, *Inorg. Chem. Commun.*, **117**, 107946 (2020); <https://doi.org/10.1016/j.inoche.2020.107946>
- N. Ahmadi, A. Nemati and M. Solati-Hashjin, *Mater. Sci. Semicond. Process.*, **26**, 41 (2014); <https://doi.org/10.1016/j.mssp.2014.04.006>
- Y. Cao, W. Yang, W. Zhang, G. Liu and P. Yue, *New J. Chem.*, **28**, 218 (2004); <https://doi.org/10.1039/b306845e>
- J.C. Yu, J. Lin and R.W. Kwok, *J. Phys. Chem. B*, **102**, 5094 (1998); <https://doi.org/10.1021/jp980332e>
- L.K. Gaur, P. Kumar, D. Kushavah, K.R. Khiangte, M.C. Mathpal, V. Agrahari, S.P. Gairola, M.A.G. Soler, H.C. Swart and A. Agarwal, *J. Alloys Compd.*, **780**, 25 (2019); <https://doi.org/10.1016/j.jallcom.2018.11.344>
- K. Kalantari, M. Kalbasi, M. Sohrabi and S.J. Royaei, *Ceram. Int.*, **43**, 973 (2017); <https://doi.org/10.1016/j.ceramint.2016.10.028>
- G. Zhu, Z. Cheng, T. Lv, L. Pan, Q. Zhao and Z. Sun, *Nanoscale*, **2**, 1229 (2010); <https://doi.org/10.1039/c0nr00087f>
- L. Jing, B. Xin, F. Yuan, L. Xue, B. Wang and H. Fu, *J. Phys. Chem. B*, **110**, 17860 (2006); <https://doi.org/10.1021/jp063148z>
- J. Ye, B. Li, M. Li, Y. Zheng, S. Wu and Y. Han, *Acta Biomater.*, **107**, 313 (2020); <https://doi.org/10.1016/j.actbio.2020.02.036>
- J. Yu and X. Yu, *Environ. Sci. Technol.*, **42**, 4902 (2008); <https://doi.org/10.1021/es800036n>
- S.A. Waghuley, S.M. Yenorkar, S.S. Yawale and S.P. Yawale, *J. Sens. Transducers*, **79**, 1180 (2007).
- H. Kato, O. Nishikawa, T. Matsui, S. Honma and H. Kokado, *J. Phys. Chem.*, **95**, 6014 (1991); <https://doi.org/10.1021/j100168a055>
- N.V. Bhat, A.P. Gadre and V.A. Bambole, *J. Appl. Polym. Sci.*, **80**, 2511 (2001); <https://doi.org/10.1002/app.1359>
- T.K. Vishnuvardhan, V.R. Kulkarni, C. Basavaraja and S.C. Raghavendra, *Bull. Mater. Sci.*, **29**, 77 (2006); <https://doi.org/10.1007/BF02709360>
- J. Wang, S. Chen and M.S. Lin, *J. Electroanal. Chem.*, **273**, 231 (1989); [https://doi.org/10.1016/0022-0728\(89\)87016-0](https://doi.org/10.1016/0022-0728(89)87016-0)
- F. El-Tantawy, K.M. Abdelkader, F.K. Ko and Y.K. Sung, *Eur. Polym. J.*, **40**, 415 (2004); <https://doi.org/10.1016/j.eurpolymj.2003.10.013>
- S. Mofokeng, V. Kumar, R. Kroon and O. Ntwaeaborwa, *J. Alloys Compd.*, **711**, 121 (2017); <https://doi.org/10.1016/j.jallcom.2017.03.345>
- S.A. El All and G.A. El-Shobaky, *J. Alloys Compd.*, **479**, 91 (2009); <https://doi.org/10.1016/j.jallcom.2009.01.071>
- C.M. Muiva, T.S. Sathiaraj and K. Maabong, *Ceram. Int.*, **37**, 555 (2011); <https://doi.org/10.1016/j.ceramint.2010.09.042>
- D.F. Swinehart, *J. Chem. Educ.*, **39**, 333 (1962); <https://doi.org/10.1021/ed039p333>
- A.H. Omran Alkhayatt and S.K. Hussian, *Mater. Lett.*, **155**, 109 (2015); <https://doi.org/10.1016/j.matlet.2015.04.130>
- J. Li and X. Liu, *Mater. Lett.*, **112**, 39 (2013); <https://doi.org/10.1016/j.matlet.2013.08.094>
- M. Omastová, M. Trchová, J. Kovárová and J. Stejskal, *Synth. Met.*, **138**, 447 (2003); [https://doi.org/10.1016/S0379-6779\(02\)00498-8](https://doi.org/10.1016/S0379-6779(02)00498-8)
- P. Chitra, A. Muthusamy and R. Jayaprakash, *J. Magn. Magn. Mater.*, **396**, 113 (2015); <https://doi.org/10.1016/j.jmmm.2015.08.042>
- P.P. Sengupta, S. Barik and B. Adhikari, *Mater. Manuf. Process.*, **21**, 263 (2006); <https://doi.org/10.1080/10426910500464602>
- A. Beniwal and Sunny, *Sens. Actuators B Chem.*, **296**, 126660 (2019); <https://doi.org/10.1016/j.snb.2019.126660>
- D. Zhang, Z. Wu, X. Zong and Y. Zhang, *Sens. Actuators B Chem.*, **274**, 575 (2018); <https://doi.org/10.1016/j.snb.2018.08.001>
- Y. Li, M. Jiao and M. Yang, *Sens. Actuators B Chem.*, **238**, 596 (2017); <https://doi.org/10.1016/j.snb.2016.07.089>
- J. Zhang, X. Liu, S. Wu, H. Xu and B. Cao, *Sens. Actuators B Chem.*, **186**, 695 (2013); <https://doi.org/10.1016/j.snb.2013.06.063>
- T. Jiang, Z. Wang, Z. Li, W. Wang, X. Xu, X. Liu, J. Wang and C. Wang, *J. Mater. Chem. C Mater. Opt. Electron. Devices*, **1**, 3017 (2013); <https://doi.org/10.1039/c3tc00370a>